Undergraduate Research Journal

Issue 18, Volume 1, November 2025

Robustness Analysis of Least Squares-based Adaptive Cruise Control in Real-World Scenarios

Axel Muniz Tello

ACKNOWLEDGEMENTS

This was written for the Department of Applied Mathematics and the Department of Electrical Engineering and Computer Science. The article was written with Ayush Pandey.

Robustness Analysis of Least Squares-based Adaptive Cruise Control in Real-World Scenarios

Axel Muñiz Tello[1] and Ayush Pandey[2]

[1]*Department of Applied Mathematics*

[2]*Department of Electrical Engineering and Computer Science*

[1,2]*University of California, Merced*

October 24th, 2025

Abstract

As automated driving technologies such as Adaptive Cruise Control (ACC) become common in the automotive industry, the risk of chain-like crashes and degraded traffic flow increases, especially if string stability and vehicle safety is not ensured. Demonstrating and improving string stability is essential to advancing the design of ACC systems for smoother, safer, and more energy-efficient vehicle platoons. We study how parameter excitability in the regressor matrix influences accuracy and adaptability in ACC systems. When excitation is low, it reduces sensitivity and weakens parameter estimation, making the system less responsive to dynamic conditions. As a result, prediction reliability is compromised, and designing controllers that maintain string stability in actual traffic becomes difficult. We model the ACC system using an ordinary differential equation in which the acceleration of the ego vehicle depends on the spacing, relative velocity, and a constant time progress parameter. Online parameter estimation is performed using a Recursive Least Squares algorithm to capture dynamic changes. To evaluate the role of excitability in the matrix, we analyze the regressor matrix at each update step, quantifying excitability through condition numbers, and convergence of parameters. We

introduce diverse driving scenarios that simulate lead and ego vehicle interactions in real-world settings. These driving scenarios are simulated with a lead and ego vehicle velocity modeled in various scenarios: random walk in equilibrium, random walk in non equilibrium, induced curve, and aggressive lead vehicle. Our findings demonstrate that situations with little to no excitation, like random walk equilibrium, had difficulty achieving precise convergence because of a rank deficiency in the regressor matrix. Higher excitation scenarios, such as induced curves, aggressive lead drivers, and random walk (non-equilibrium), on the other hand, showed better convergence and reduced estimation error. In highway scenarios with extended constant speeds, limited excitation was also noted, which resulted in degraded trajectory prediction, parameter drift, and ill-conditioned regressors. In contrast, mixed-driving conditions with periodic excitation showed improved performance, maintaining estimator stability over long periods of time. Overall, these findings show that sustained excitation reflecting realistic traffic variability is necessary for both strong ACC performance and precise online parameter estimation in these driving scenarios.

1.0 Introduction

Cruise control technologies have become a heavily utilized tool in the automotive and transportation industries. Companies such as Toyota, Tesla, and Mercedes-Benz have integrated these systems into their vehicles and further developed them into Adaptive Cruise Control (ACC) systems. In ACC systems, the ego vehicle dynamically adjusts its speed to maintain a desired spacing from the lead vehicle, accounting for relative velocity and road conditions. Unlike conventional cruise control, which holds a constant driver-set speed, ACC adapts to changing traffic dynamics, enabling smoother and more efficient autonomous driving. ACC systems overall have shown to bring improved roadway safety, traffic efficiency, and energy conservation Zhang et al. (2025) on roadways.

However, ACC systems remain constrained by inadequate sensor perception of individual vehicle dynamics Luo (2023), which limits their capacity to accurately interpret surrounding drivers' behavior. When ACC systems are unable to effectively learn and interpret these dynamics, string

instability may arise. String instability refers to the propagation, and amplification of velocity perturbations along a vehicle platoon, leading to potential crashes, chain-like collisions, and degraded traffic flow in high-density environments Zhang et al. (2025).

ACC systems are often described using the Constant Time Headway (CTH) model, formulated as an ordinary differential equation (ODE) governing the acceleration of an ego vehicle based on spacing and relative velocity Wang, Gunter, Nice, Monache, and Work (2021). The parameters are estimated online using Recursive Least Squares (RLS), where estimation quality depends on the excitation of the regressor matrix Wang, Gunter, and Work (2020). Poorly excited or ill-conditioned regressor matrices limit parameter observability, resulting in slow convergence and inaccurate model adaptation Tsuruhara and Ito (2025).

The ability of ACC systems to autonomously learn and adapt to nonlinear vehicle dynamics in real-world scenarios is rarely demonstrated by current studies Tsuruhara and Ito (2025); Wang et al. (2021, 2020), despite a wealth of modeling and parameter estimation research. While actual driving is frequently noisy, fleeting, and weakly excited, most analyses assume environments that are consistently excited or well-conditioned Luo (2023); Wang et al. (2020). In order to close that gap, this paper experimentally validates RLS-based parameter estimation in a variety of driving scenarios, emphasizing the effects of noise and regressor excitation on estimation reliability. Beyond idealized simulations, this work expands our understanding of ACC adaptability and robustness by testing under real-world, high-variability traffic conditions.

2.0 Related Work

Several past works have applied RLS for online parameter estimation in ACC models Tsuruhara and Ito (2025); Wang et al. (2021). While these methods have proven effective under controlled or ideal conditions, they often assume persistent excitation and simplified vehicle dynamics Wang et al. (2020). In practice, real-world driving does not always satisfy these assumptions. Factors such as noisy sensor data, transient maneuvers, and nonlinear driver vehicle interactions degrade

estimation accuracy and slow convergence.

Additional studies have attempted to mitigate these issues by introducing modified versions of RLS algorithms, such as two-layered or forgetting-factor variants Tsuruhara and Ito (2025). However, their performance remains limited under unstructured driving conditions. This motivates further investigation into adaptive estimation schemes capable of learning dynamic vehicle behavior across multiple driving scenarios in real time while maintaining robustness to poor excitation and sensor noise.

3.0 Preliminaries

This section outlines the mathematical frameworks and notation used throughout this research. We first describe the CTH model that governs the follower's vehicle dynamics, string stability and persistent excitation, and finite excitation, followed by a basic review of RLS algorithm for online system parameter estimation. Wang et al. (2021)

3.0.1 CTH model

The ACC system is modeled by the CTH principle which maintains a desired spacing proportional to the follower's velocity Gunter, Janssen, Barbour, Stern, and Work (2020). The overall dynamics can be expressed as:

$$\dot{v}(t) = f(\boldsymbol{\theta}, s(t), v(t), \Delta v(t)) = \alpha(s(t) - \tau v(t)) + \beta(\Delta v(t)), \quad \boldsymbol{\theta} \in \mathbb{R}^3 \tag{1}$$

where $s(t)$, $v(t)$, and $\Delta v(t)$ are the space gap, velocity, and velocity difference between the ACC and the lead vehicle. The parameter vector

$$\boldsymbol{\theta} = [\, \alpha \; \beta \; \tau \,]^\top \tag{2}$$

controls the gain on the CTH term, and the relative velocity term respectively, while the

parameter τ is the time gap at equilibrium Wang et al. (2021). Compared to all the modeling choices, it is observed that CTH-RV is the common model in terms of fitting the data computationally compared to more nonlinear complex systems Tsuruhara and Ito (2025).

3.0.2 String stability

String stability ensures that disturbances in the motion of the vehicle does not amplify downstream to the rest of the vehicles Luo (2023). Physically, string instability is exhibited as the "stop and go" oscillations in a vehicle's motion. Velocity perturbations grow exponentially, and so do traffic waves form in the form of traffic.

We measure string stability for the CTH-RV model using parameters α, β, τ under theoretical conditions. The vehicle dynamics are linearized around a steady-state spacing and velocity will yield frequency-domain inequalities that determine whether physical disturbances are diminished or heightened Wang et al. (2021). Particularly, the system is said to be L^2 string stable if

$$\alpha^2\tau^2 + 2\alpha\beta\tau - 2\alpha \geq 0 \tag{3}$$

and is L^∞ string stable if

$$(\alpha\tau + \beta)^2 - 4\alpha \geq 0 \tag{4}$$

The L^2 condition ensures that the total energy diminishes along the platoon, and the L^∞ will ensure that the instantaneous peaks don't amplify further Wang et al. (2021).

3.0.3 Recursive least squares

Adaptive Cruise Control systems are excellent in operating in diverse, high-variability scenarios. Since our estimation must be accurate, it must be done so using online methods; meaning that the estimations are accurately predicted while new data keeps coming in Wang et al. (2021). Since our estimations must be accurate and precise, the RLS algorithm provides a great foundation, updating

itself as new information keeps coming in.

RLS is reliable because it continuously updates parameter estimates in real time using all possible available data, ensuring rapid convergence and low estimation error. In addition to maintaining numerical stability through the recursive structure, it can adjust its estimations due to the forgetting factor Tsuruhara and Ito (2025). Moreover, at the center of this approach, it seeks to minimize the cumulative squared prediction between the measured acceleration, and the predicted acceleration while recursively updating our model's $\boldsymbol{\theta}$ parameter and modeled similar to simulations in Wang et al. (2021) yields,

$$\hat{\gamma}_k = \hat{\gamma}_{k-1} + \boldsymbol{P_k X_k}(\boldsymbol{Y_k} - \hat{\gamma}_{k-1}\boldsymbol{X_k}) \tag{5}$$

Where $\boldsymbol{P}_k$ is the covariance matrix at the k-th step, $\boldsymbol{X}$ is the regressor matrix which holds all vehicle velocity and space gap information, and finally, $\boldsymbol{Y}$ which contains the measured acceleration at the k-th step.

4.0 Driving Scenarios

We analyze the computational robustness, and reliability of the RLS algorithm by simulating 4 realistic scenarios with high possibility of existence in real-life. These driving scenarios, serve as tests that we will use to analyze the RLS algorithm when attempting to recover the $\boldsymbol{\theta}$ model parameter. We want to quantify how accurate our RLS algorithm can be under scenarios that can help us quantify the robustness and safety of ACC systems.

4.0.1 Case 1: Random walk

First case we seek to simulate and quantify are two vehicles, a lead vehicle $\underline{u}(t) \in \mathbb{R}^n$ and a follower-ego vehicle, $\underline{v}(t) \in \mathbb{R}^n$. We assume that both vehicles assume normal driving conditions on a highway. Moreover, we assume that there are no other surrounding vehicles on the highway, and we let these two vehicles drive on the highway for 900 time steps (or seconds). RLS can be

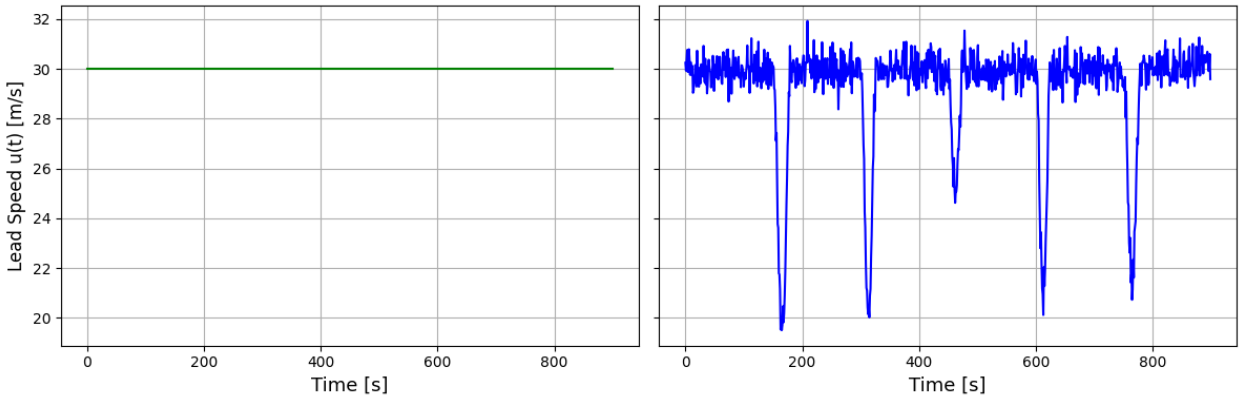

Figure 1: *Left plot shows the constant-speed sub case, while the right illustrates the non-equilibrium case of our scenario.*

evaluated using two sub test cases to evaluate how well RLS can estimate model parameters on two conditions:

1. We test RLS under equilibrium assuming that there is no acceleration meaning that their relative speeds are constant, $v_k = u_k = 0$

2. Second sub case we test is RLS under non-equilibrium conditions, meaning that the lead vehicle has non constant speeds with added fluctuations and drops in speeds, $v_k = u_k \neq 0$

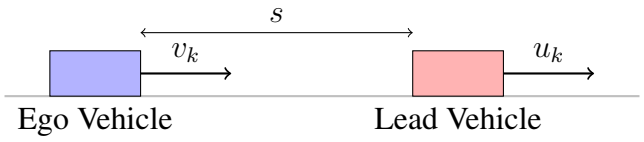

Figure 2: *Two cars on a straight road, separated by distance s.*

4.0.2 Case 2: Induced road curve

Second case we seek to simulate our same two vehicle $\underline{u}(t)$ and $\underline{v}(t)$; however, the changes that we apply to this case is that we drive these vehicles from the highway to a steep curve. We seek to test the robustness of the RLS algorithm under induced road curve. This case is quite applicable in real life situations where we have geography that can be steep and curved; we want to quantify the estimation accuracy of RLS under this condition.

Moreover, there exists an exception when it comes to the the case we seek to simulate and evaluate. Physically, we are unable to simulate two vehicles going at constant speeds, this would imply that the vehicles would fall off the curved road and harm the drivers and passengers. Therefore, this case only considers simulating a non-equilibrium scenario where, $u_k = v_k \neq 0$

1. RLS under non-equilibrium non constant speeds (with added fluctuations and drops in speeds to simulate curve).

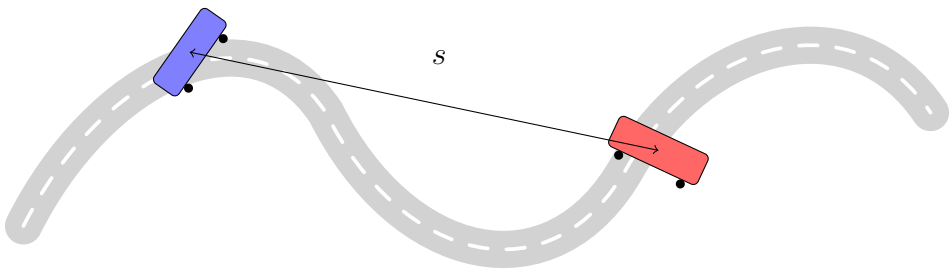

Figure 3: *Visualization of curved road with a lead and follower vehicle.*

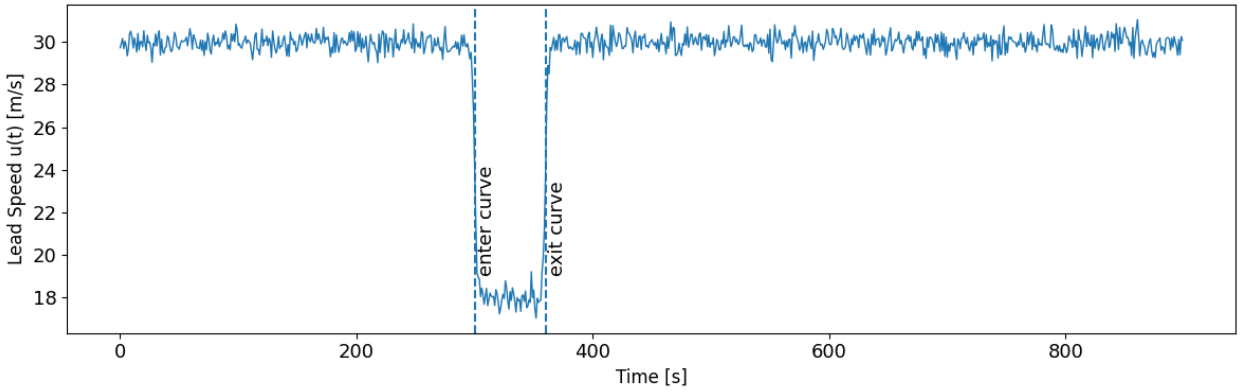

Figure 4: *Plot describes motion of the lead vehicle $u(t)$ in a curve for our scenario.*

4.0.3 Case 3: Aggressive lead vehicle

In this fourth and final scenario that we want to simulate, we will still have our too vehicles, $\underline{u}(t)$ and $\underline{v}(t)$; however, what would change in this scenario is that we will have these two vehicles who

will be driving on a highway. However, what we will be testing is the RLS capacity to recover the α, β, τ and parameters with an aggressive lead vehicle.

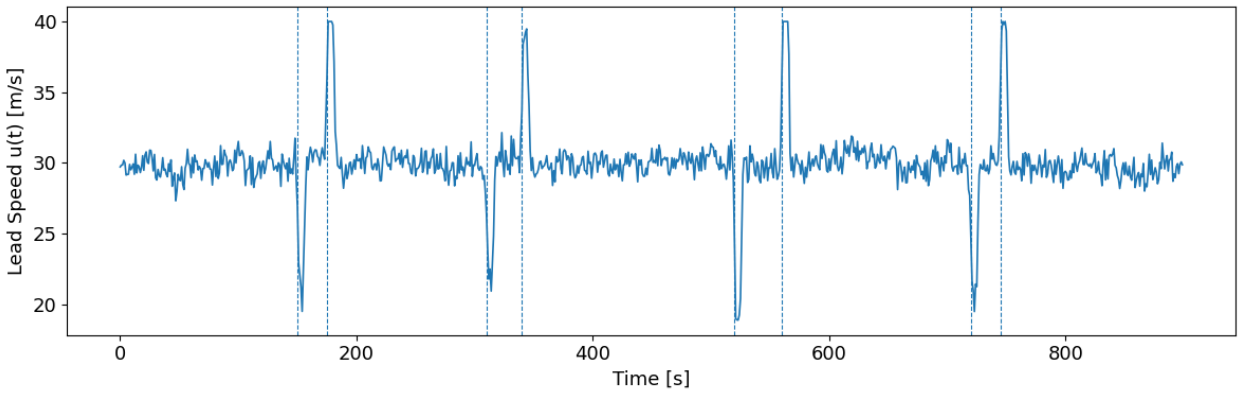

Figure 5: *Plot describing vehicle motion with an aggressive lead vehicle*

1. RLS under non-equilibrium non-constant speeds (with added fluctuations in speeds) with road hazards.

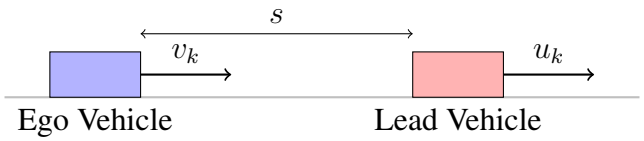

Figure 6: *Two cars on a straight road, separated by distance s.*

5.0 Methodology

This section presents theoretical derivations of the RLS algorithm, the dataset generation procedure, the simulation setup, and the evaluation metrics used throughout this study.

5.0.1 Recursive least squares derivation

Recall our CTH-RV model from Wang et al. (2021)

$$\dot{v}(t) = f(\boldsymbol{\theta}, s(t), v(t), \Delta v(t)) = \alpha(s(t) - \tau v(t)) + \beta(\Delta v(t)), \qquad \boldsymbol{\theta} = [\alpha, \beta, \tau]^\top \tag{6}$$

we take the same similar approach from Wang et al. (2021) to derive our RLS estimator. We are able to take that same model and rewrite it using Euler's forward step scheme Burden Richard (2022):

$$v_{k+1} = v_k + \alpha(s_k - \tau v_k)\Delta T + \beta(u_k - v_k)\Delta T \tag{7}$$

where v_k, s_k, and u_k is the velocity of the follower vehicle, the space gap, and the lead vehicle velocity at timestep k. The term ΔT is the timestep size which is chosen to correspond to the frequency at which the velocity, space gap, and relative velocity is measured at. For this study, we set ΔT to be on the order of 1/20 of a second.

The vehicle dynamics can be rewritten as:

$$v_{k+1} = \gamma_1 v_k + \gamma_2 s_k + \gamma_3 u_k \tag{8}$$

where,

$$\gamma_1 := (1 - (\alpha\tau + \beta)\Delta T), \gamma_2 := \alpha\Delta T, \gamma_3 := \beta\Delta T$$

We follow the approach in Wang et al. (2021), but instead of estimating the individual parameters obtained by inverting $\hat{\gamma}$ to recover α, β, and τ, we directly estimate $\gamma_1, \gamma_2, \gamma_3$. This lets us demonstrate that the vector $\hat{\gamma} = [\gamma_1, \gamma_2, \gamma_3]^\top$ can be recovered from the same experimental dataset used in Wang et al. (2021), namely (v_k, s_k, u_k) for all $k \in 1, 2, \ldots, K$. By stacking the uniformly sampled sensor measurements, we obtain:

$$\begin{bmatrix} v_2 \\ v_3 \\ \vdots \\ v_k \end{bmatrix} = \begin{bmatrix} v_1 & s_1 & u_1 \\ v_2 & s_2 & u_2 \\ \vdots & \vdots & \vdots \\ v_{k-1} & s_{k-1} & u_{k-1} \end{bmatrix} \begin{bmatrix} \gamma_1 \\ \gamma_2 \\ \gamma_3 \end{bmatrix} \tag{9}$$

or,

$$\boldsymbol{Y} = \boldsymbol{X}\gamma$$

In this experiment, the vector $\boldsymbol{Y}$ will contain all of the values v_k from timestep 2 to K. The matrix $\boldsymbol{X}$ will contain the collection of the follower velocity, space gap, and lead velocity from timestep 1 to $K-1$. Finally, the vector $\boldsymbol{\gamma}$ represents the set of γ values used to solve for the model parameters.

Before we are able to determine that there exists a solution for our least squares problem we must note that there will only be a solution to this system of equation if rank(X) = rank([X, Y]) = 3. Moreover, this condition is not satisfied at equilibrium where $v_i = v_j = u_k$ for all time steps i, j, and k. In other words, since $\boldsymbol{X} \in \mathbb{R}^{m\times 3}$ and two of its columns are identical $v_k = u_k$, the column rank is not 3, but 2 because the columns are not linearly independent. Mathematically:

$$\text{rank}(\boldsymbol{X}) = \dim(\text{col}(\boldsymbol{X})) = 2$$

Since an online estimation method is desired, we convert the least squares problem into a recursive online method using the Recursive Least Squares (RLS) algorithm to recursively estimate our $\hat{\gamma}$ vector as:

$$\hat{\gamma}_k = \hat{\gamma}_{k-1} + \boldsymbol{P_k}\boldsymbol{X_k}(\boldsymbol{Y_k} - \hat{\gamma}_{k-1}\boldsymbol{X_k}) \tag{10}$$

where $P_k^{-1} = \sum_{i=1}^{k} X_i X_i^T$ is the cumulative outer product of X_k, commonly referred to as the Gram matrix. In order to solve (16) we are going to need an initial estimate of the parameters $\gamma_0 \sim \mathcal{N}(\hat{\gamma_0}, P_0)$.

5.0.2 Numerical implementation

To enable real-time parameter estimation of the CTH–RV model under various driving conditions (scenarios), the RLS estimator developed in the previous section was implemented in Python. We can examine how data conditioning affects the convergence of $\hat{\gamma}_k$ across all environments since each scenario offers a unique excitation profile for the regressor matrix $\boldsymbol{X}_k$.

This is the manner in which the pipeline for numerical simulation is constructed. The lead velocity u_k, follower velocity v_k, and space gap s_k are sampled or generated based on the given

driving scenario at each discrete time step k. The regressor $\boldsymbol{X}_k = [v_k, s_k, u_k]^\top$ and the target $Y_k = v_{k+1}$ are formed by these signals. After that, the RLS algorithm modifies its parameter estimate in accordance with

$$\hat{\gamma}_k = \hat{\gamma}_{k-1} + \boldsymbol{P}_k \boldsymbol{X}_k \big(Y_k - \boldsymbol{X}_k^\top \hat{\gamma}_{k-1}\big),$$

with $\boldsymbol{P}_k^{-1} = \sum_{i=1}^{k} \boldsymbol{X}_i \boldsymbol{X}_i^\top$ serving as the Gram matrix that quantifies data excitation.

We calculate the condition number $\kappa(\boldsymbol{X}_k^\top \boldsymbol{X}_k)$ and track the change of the estimated parameters $\hat{\gamma}_k$ over time in order to evaluate the numerical stability of RLS under various excitation regimes. Usually seen during near-equilibrium motion, poorly conditioned matrices cause unstable parameter updates and high κ values. On the other hand, well-conditioned regressors and smooth convergence are produced in dynamic driving scenarios with rich excitation.

Previous research has demonstrated that adding a preconditioner matrix $\boldsymbol{Q}_k$ can lower numerical condition numbers and increase stability under weak excitation, even though it was not used in this study Rørtveit and Husøy (2009). Future implementations could use this change to lessen drift from ill-conditioning and further regulate the growth of $\boldsymbol{P}_k$.

6.0 Results

We present the results from applying the Recursive Least Squares (RLS) estimator to the four driving scenarios described in Section 4. Each experiment examines the effect of excitation and matrix conditioning on the convergence of the estimated parameter vector $\hat{\gamma}_k$ and evaluates the impact of excitability on numerical stability and estimation accuracy. You can find our results in the accompanying GitHub repository.

6.0.1 Case 1: Random walk (equilibrium)

Simulating our data for a total of $K = 900$ steps for $u_k \sim$ CTH-RV Model, and letting $v_k \sim \mathcal{N}(\mu = 0, \sigma^2 = 0.05^2)$ we are able to obtain and visualize our model as:

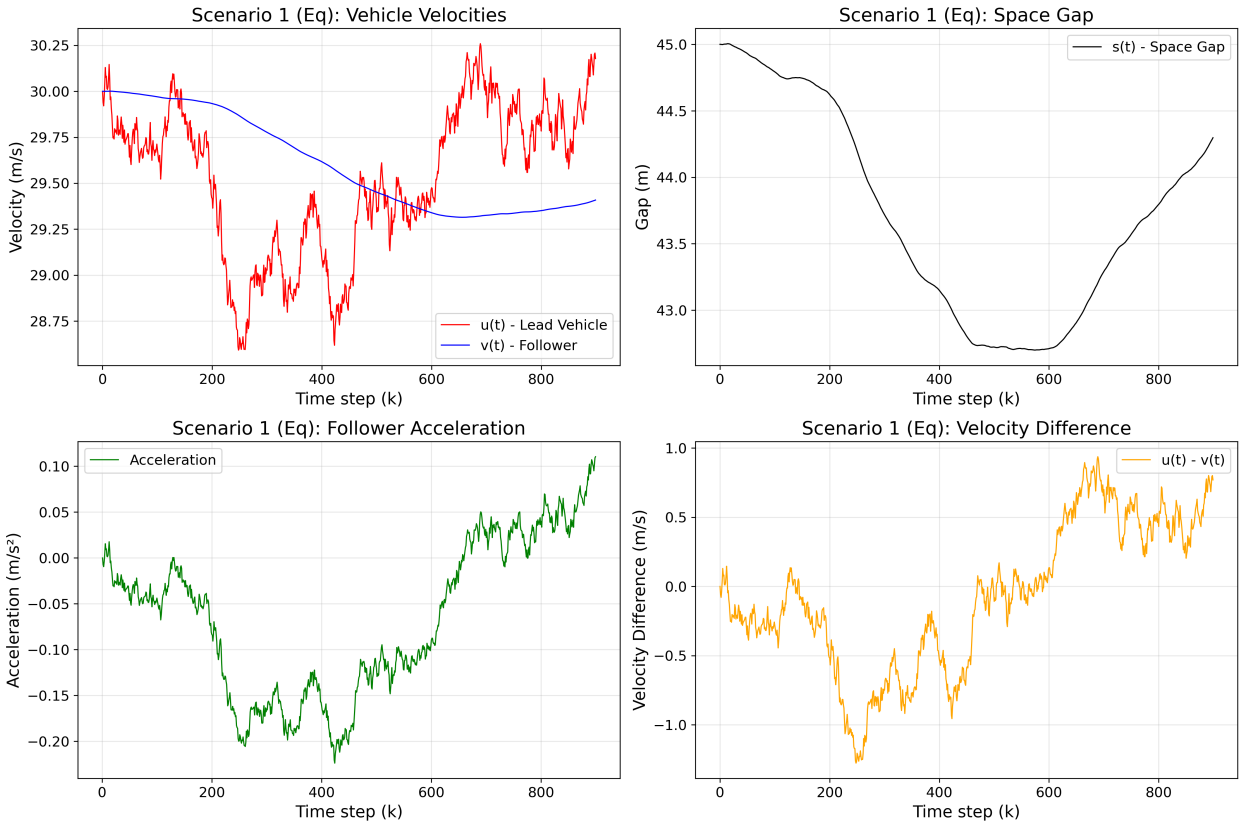

Figure 7: *Data analysis for case 1 (Equilibrium), models vehicle velocities, space gap, follower acceleration, and velocity difference*

From the dataset that we generated, we obtain our condition number of $\mathcal{K}(\boldsymbol{A}^\top \boldsymbol{A}) = 1.05 \times 10^5$

Parameter	Expected	Predicted	Error
α	0.08	0.069	0.011
β	0.12	0.090	0.030
τ	1.50	1.520	-0.020

Table 1: *Expected vs. predicted parameter values (error* $= \hat{\gamma} - \gamma$*)*

Since this matrix is ill-conditioned it demonstrates that the regressor matrix is not being persistently excited, which this translates to low variance in our $\underline{u}(t)$ velocity profile. This is modeled through

our results of convergence, our RLS estimation algorithm proves that it struggles to converge from $[0, K]$ rather it converges after 900 steps. RLS struggles to converge under in our scenario that tests robustness within our sample size.

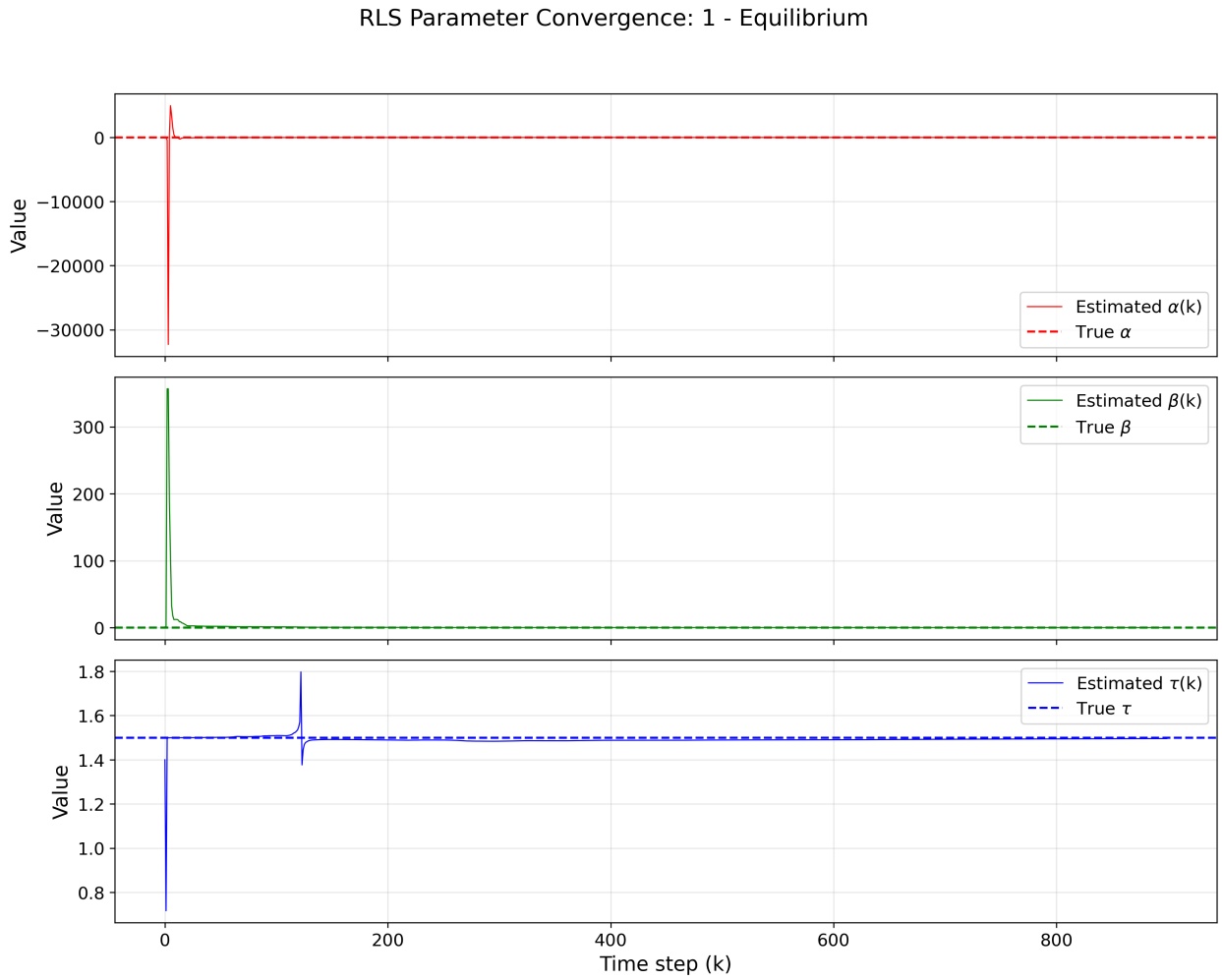

Figure 8: *Convergence plot of α, β, τ in scenario 1 under equilibrium.*

6.0.2 Case 1: Random walk (Non equilibrium)

For the other counterpart of this first scenario we generate our data where $v_k = u_k \neq 0$ and generate our data for $u_k \sim$ CTH-RV Model, and letting $v_k \sim \mathcal{N}(\mu = 0, \sigma^2 = 0.5^2)$, our data is modeled as with our condition number of $\mathcal{K}(\boldsymbol{A}^\top \boldsymbol{A}) = 1.02 \times 10^3$:

The convergence of the parameters are modeled and shown, demonstrating that while the

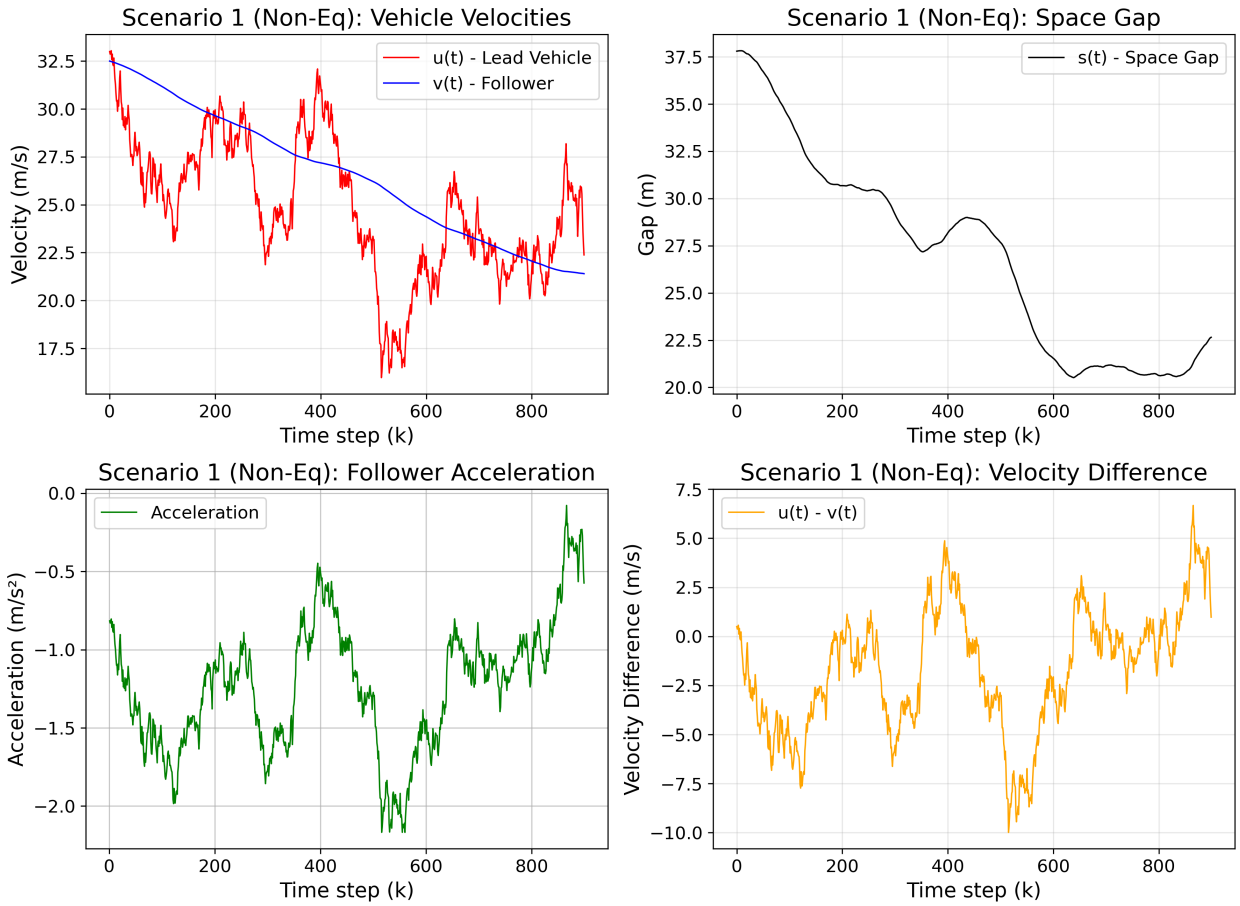

Figure 9: *Data analysis for case 1 (Non Equilibrium), models vehicle velocities, space gap, follower acceleration, and velocity difference*

Parameter	**Expected**	**Predicted**	**Error**
α	0.08	0.082	-0.002
β	0.12	0.121	-0.001
τ	1.50	1.505	-0.005

Table 2: *Expected vs. predicted parameter values (error* $= \hat{\gamma} - \gamma$*)*

condition number of our matrix is one order of magnitude smaller than our equilibrium case, it begins to perform better with higher variance in our dataset generation.

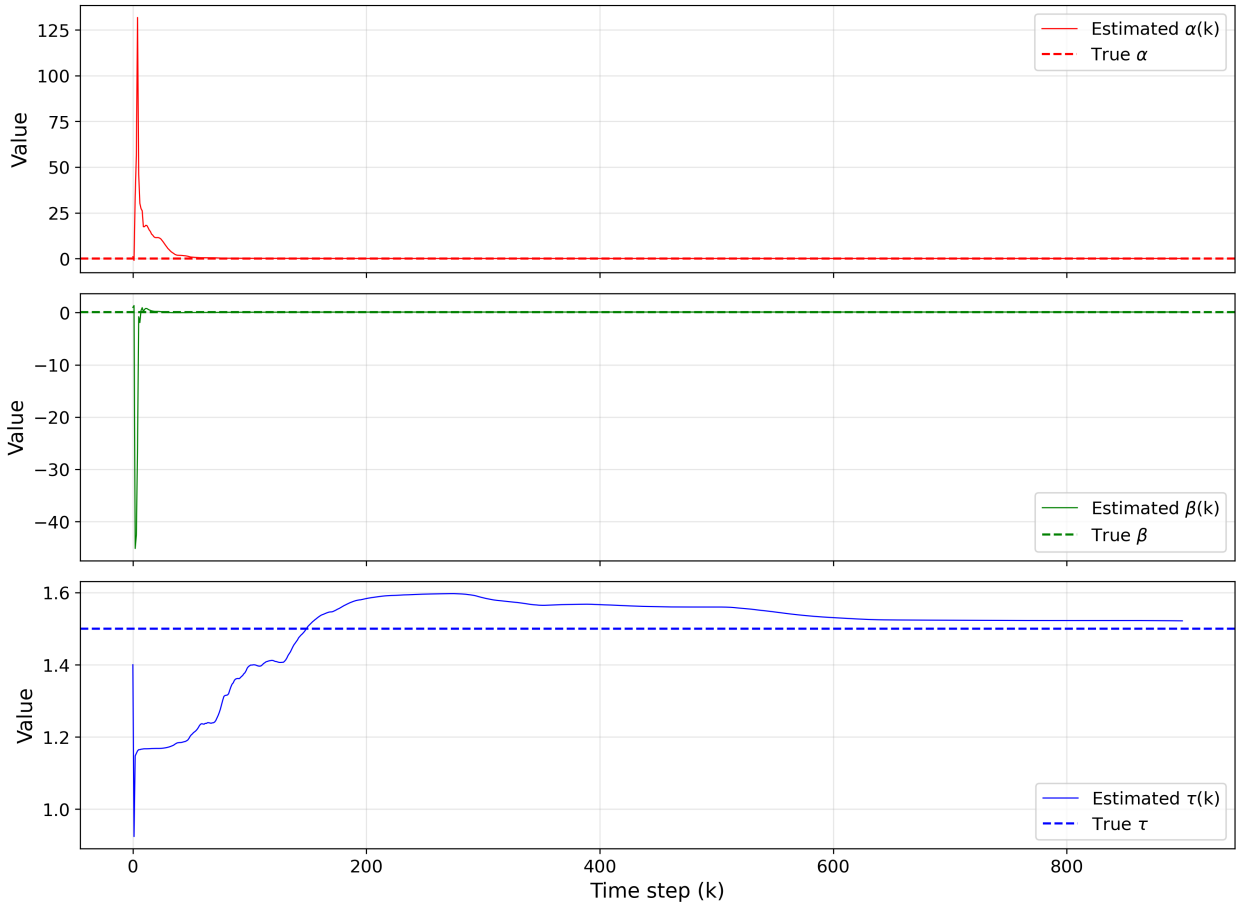

Figure 10: *Convergence plot of α, β, τ, in case 1 (Non equilibrium)*

6.0.3 Case 2: Induced road curve

After describing how the estimator performs under both equilibrium and non-equilibrium random-walk scenarios, we now examine a more structured setup. Case 2 introduces an induced road-curve scenario to study how deterministic velocity fluctuations affect matrix conditioning and parameter convergence. The follower vehicle's velocity profile is generated according to

$$u_t[i] = u_0 - (u_0 - u_{\min}) \exp\left(-\frac{(i-c)^2}{2\sigma^2}\right),$$

where u_0 is the initial velocity, $u_{\min}$ is the minimum speed at the curve center, c is the curve's center index, and σ controls the curve width. The lead vehicle's velocity follows the CTH-RV

model, $v_k \sim$ CTH-RV.

This setup induces both vehicles to decelerate sharply and maintain safe spacing, allowing the RLS estimator to track parameters efficiently under nonlinear excitation. The generated dataset is shown below.

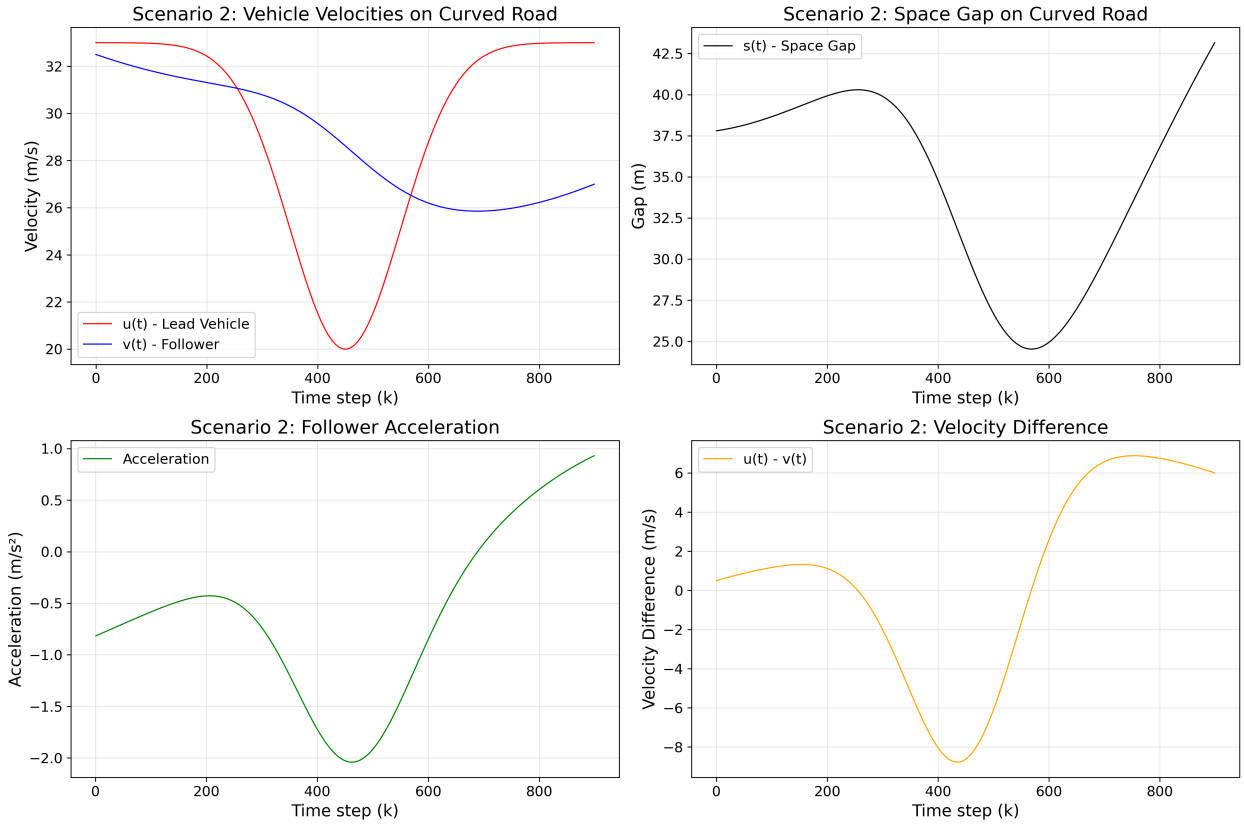

Figure 11: *Data Analysis for case 2, modeling vehicle velocities, space gap, follower acceleration, and velocity difference*

The corresponding convergence behavior of the estimated parameters is shown in Figure 12 with our condition number $\mathcal{K}(A^\top A) = 3.68 \times 10^2$.

Parameter	**Expected**	**Predicted**	**Error**
α	0.08	0.081	-0.001
β	0.12	0.119	0.001
τ	1.50	1.503	-0.003

Table 3: *Expected vs. predicted parameter values (error* $= \hat{\gamma} - \gamma$*)*

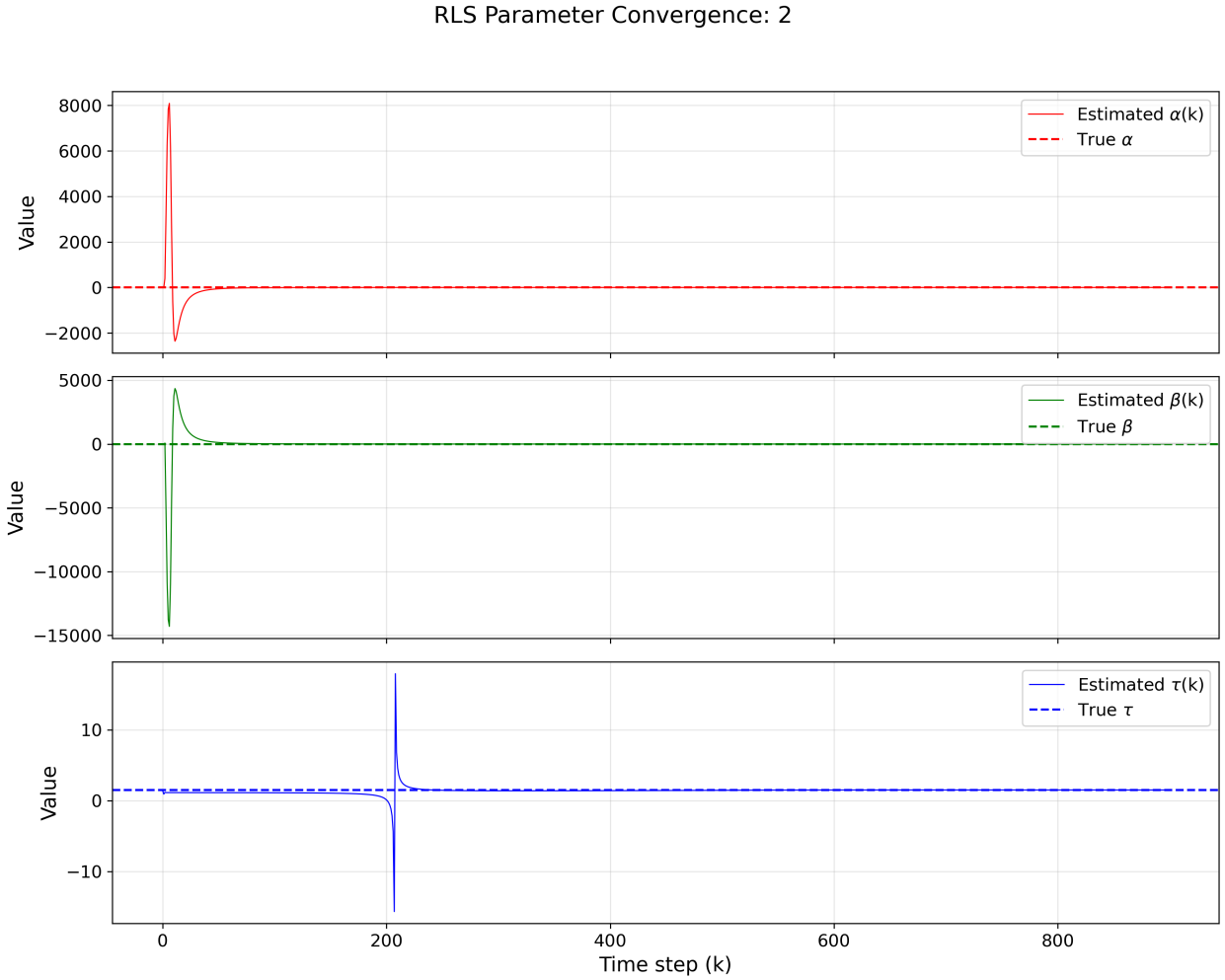

Figure 12: *Convergence plot of α, β, τ for scenario 2: Induced Road Curve.*

6.0.4 Case 3: Aggressive lead driver

Finally, in order to simulate aggressive driving in congested traffic, this scenario puts the estimator under stress from sudden, high-jerk maneuvers from the lead car, abrupt stopping, fast accelerations, and little rest times between events. In contrast to the smoother excitation in Cases 1-3, the input in this case is heavy-tailed and intermittent, resulting in brief windows of high (nonstationary) excitation and transient spikes in the regressor's conditioning.

The RLS estimator's robustness to outliers and sudden shifts, its susceptibility to transient ill-conditioning, and the impact of such occurrences on convergence and parameter drift are all assessed using this instance.

Specifically, we investigate how the forgetting factor balances responsiveness and noise amplification, and if fast excitation bursts enhance Identifiability without destabilizing the updates. Below is a report on the convergence behavior and generated data for this configuration.

Our u_k is still generated from the CTH-RV model, and $v_k \sim \mathcal{N}(\mu = 0, \sigma^2 = 0.3^2)$ as follows:

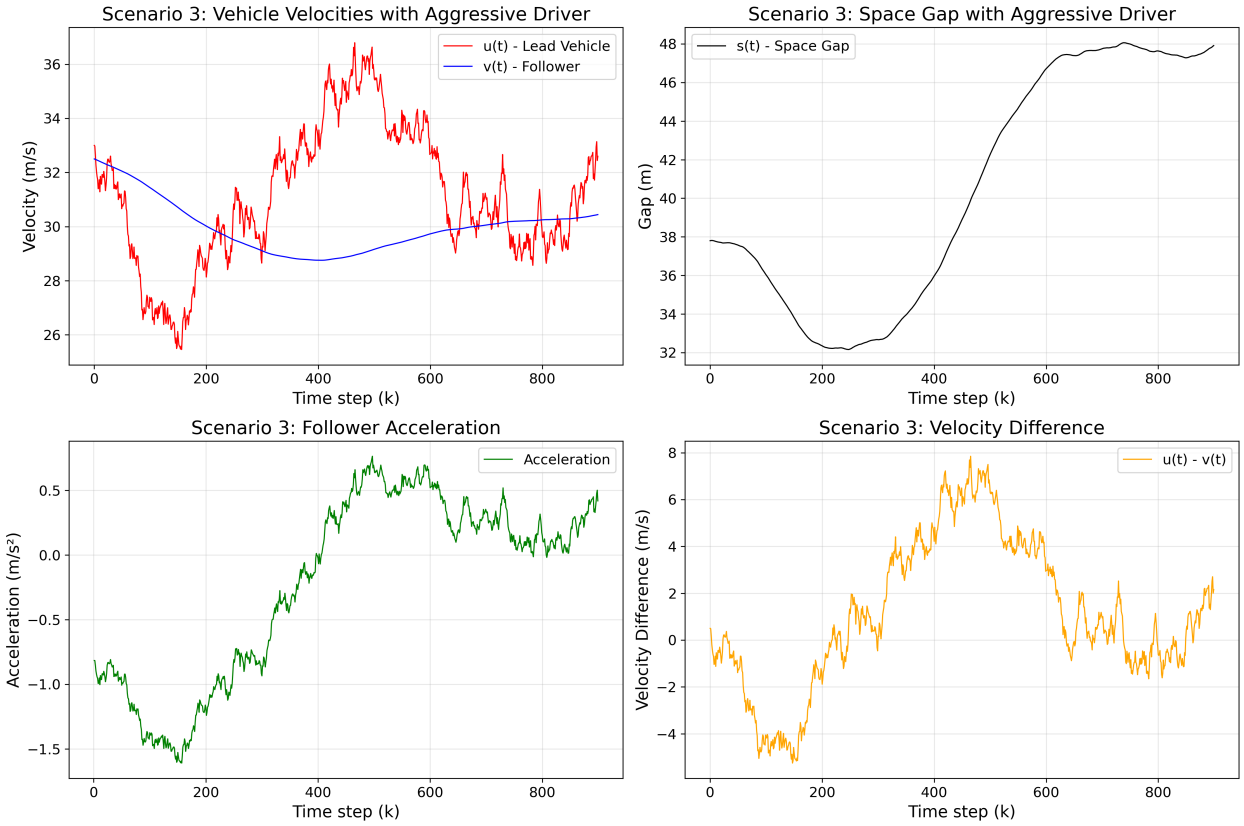

Figure 13: *Data analysis for case 3, modeling vehicle velocities, space gap, follower acceleration, and velocity difference*

And our convergence plots with our conditional number being $\mathcal{K}(X^\top X) = 7.39 \times 10^2$.

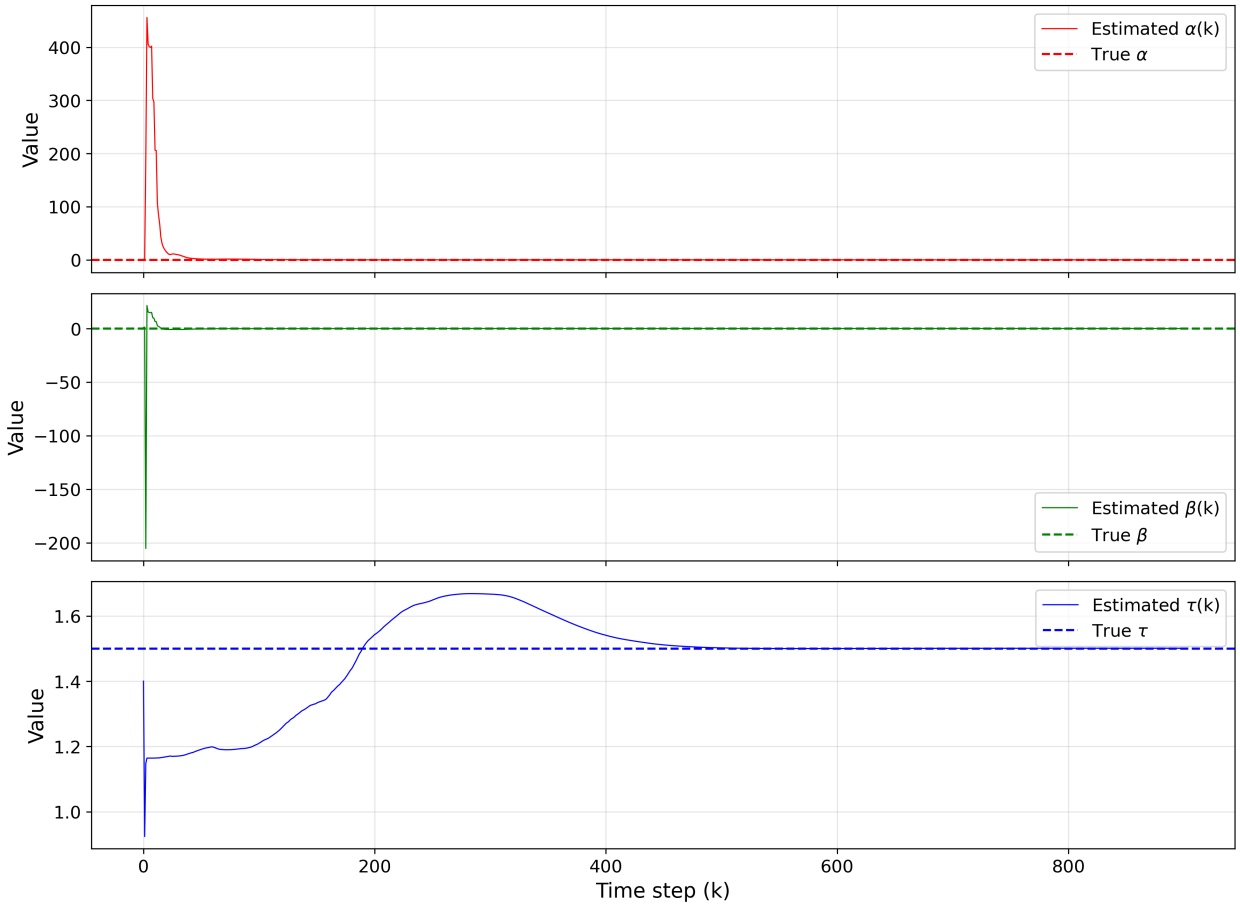

Figure 14: *Convergence plot of α, β, τ for scenario 3*

Parameter	**Expected**	**Predicted**	**Error**
α	0.08	0.081	-0.001
β	0.12	0.12	0.00
τ	1.50	1.501	-0.001

Table 4: *Expected vs. predicted parameter values (error $= \hat{\gamma} - \gamma$)*

7.0 Discussion

The overall outcomes for each of the three driving scenarios demonstrate how sensitive RLS is to the excitation level and the conditioning of the regressor matrix in real-world conditions. In low-excitation conditions, like the equilibrium random-walk scenario, inadequate conditioning resulted in higher parameter drift and slower convergence. The estimator showed faster and more consistent convergence when the excitation grew, either by stochastic variation or by structured maneuvers such as the induced road curve, or aggressive lead vehicle. These patterns support the idea that numerical conditioning and continuous excitation are necessary for effective RLS performance under these driving scenarios.

8.0 Conclusion

The robustness of RLS was investigated in this work in three representative driving scenarios with different excitation and matrix conditioning levels. The findings show that the degree of persistent excitation in the regressor data has a significant impact on estimator accuracy and convergence speed. While stronger excitation, introduced through random or structured velocity variations, significantly improved stability and estimation accuracy, weak excitation caused the estimator to converge slowly and exhibit minor parameter drift due to ill-conditioning.

These results highlight how crucial it is to keep the excitation of the model high enough for accurate real-time parameter estimation in vehicle-following scenarios. Prior research has also indicated that adding a preconditioner matrix $\boldsymbol{Q}_k$ could further lower numerical condition numbers and improve robustness under weakly excited situations, even if preconditioning was not used in the current implementation Tsuruhara and Ito (2025); Wang et al. (2021). Future research will concentrate on evaluating the RLS algorithm using increasingly intricate, real-world driving information along with integrating such numerical stabilization techniques.

References

Burden Richard, B. A., Faires Douglas. (2022). *Numerical analysis*. Cengage.

Gunter, G., Janssen, C., Barbour, W., Stern, R. E., & Work, D. B. (2020, Mar). Model-based string stability of adaptive cruise control systems using field data. *IEEE Transactions on Intelligent Vehicles*, *5*(1), 90–99. doi: 10.1109/tiv.2019.2955368

Luo, T. (2023). Study on adaptive cruise control systems of passenger vehicles and solutions based on v2x technologies. In *2023 4th international conference on computer engineering and intelligent control (icceic)* (p. 539-549). doi: 10.1109/ICCEIC60201.2023.10426734

Rørtveit, L., & Husøy, J. H. (2009). A new prewhitening-based adaptive filter which converges to the wiener-solution. In *2009 conference record of the forty-third asilomar conference on signals, systems and computers* (p. 1360-1364). doi: 10.1109/ACSSC.2009.5469890

Tsuruhara, S., & Ito, K. (2025). *Discrete-time two-layered forgetting rls identification under finite excitation.* Retrieved from `https://arxiv.org/abs/2504.19518`

Wang, Y., Gunter, G., Nice, M., Monache, M. L. D., & Work, D. B. (2021). Online parameter estimation methods for adaptive cruise control systems. *IEEE Transactions on Intelligent Vehicles*, *6*(2), 288-298. doi: 10.1109/TIV.2020.3023674

Wang, Y., Gunter, G., & Work, D. B. (2020). Online parameter estimation of adaptive cruise control models with delays and lags. In *2020 ieee 23rd international conference on intelligent transportation systems (itsc)* (p. 1-6). doi: 10.1109/ITSC45102.2020.9294538

Zhang, C., Guo, H., Wang, Z., Feng, F., Pradhan, A., & Bao, S. (2025). *Assessing the effectiveness of driver training interventions in improving safe engagement with vehicle automation systems.* Retrieved from `https://arxiv.org/abs/2509.25364`